

Article

# Third-Order Nonlinear Spectrum of GaN under Femtosecond-Pulse Excitation from the Visible to the Near Infrared

Gustavo F. B. Almeida<sup>1,2</sup>, Sabrina N. C. Santos<sup>1</sup>, Jonathas P. Siqueira<sup>1</sup>, Jessica Dipold<sup>1</sup>, Tobias Voss<sup>3</sup> and Cleber R. Mendonça<sup>1,\*</sup> 

<sup>1</sup> São Carlos Institute of Physics, University of São Paulo PO Box 369, 13561-970 São Carlos, SP, Brazil; gustavo.foresto.almeida@alumni.usp.br (G.F.B.A.); sabrinancs@usp.br (S.N.C.S.); jonathasusp@ursa.ifsc.usp.br (J.P.S.); jessica.dipold@usp.br (J.D.)

<sup>2</sup> Institute of Physics, Federal University of Uberlândia, PO Box 593, 38400-902 Uberlândia, MG, Brazil

<sup>3</sup> Institute of Semiconductor Technology and Laboratory for Emerging Nanometrology LENA, Technische Universität Braunschweig, 38106 Braunschweig, Germany; tobias.voss@tu-braunschweig.de

\* Correspondence: crmendon@ifsc.usp.br; Tel.: +55-16-3373-8085

Received: 18 May 2019; Accepted: 15 June 2019; Published: 18 June 2019



**Abstract:** Gallium nitride (GaN) has been established as a promising candidate for integrated electro-optic and photonic devices, aiming at applications from optical switching to signal processing. Studies of its optical nonlinearities, however, lack spectral coverage, especially in the telecommunications range. In this study, we measured the two-photon absorption coefficient ( $\beta$ ) and the nonlinear index of refraction ( $n_2$ ) of GaN from the visible to the near-infrared by using femtosecond laser pulses. We observed an increase of  $\beta$  from  $(1.0 \pm 0.2)$  to  $(2.9 \pm 0.6) \times 10^{-11}$  m/W as the photon energy approached the band gap from 1.77 up to 2.25 eV (700–550 nm), while  $n_2$  varied from  $(90 \pm 30) \times 10^{-20}$  up to  $(265 \pm 80) \times 10^{-20}$  m<sup>2</sup>/W within a broad spectral range, from 0.80 up to 2.25 eV (1550–550 nm). The results were modeled by applying a theory based on the second-order perturbation theory and the Kramers-Kronig relationship for direct-gap semiconductors, which are important for the development of GaN-based nonlinear photonic devices.

**Keywords:** gallium nitride; nonlinear optics; nonlinear spectroscopy; femtosecond laser

## 1. Introduction

The wide-bandgap direct-gap semiconductor gallium nitride (GaN) is well-known for its excellent electronic and linear optical properties [1–3] that have resulted in a large variety of electronic and optoelectronic applications, such as light-emitting diodes (LEDs) [4], field-effect transistors (FETs) [5,6], and high-temperature electronic devices [7]. Throughout the years, outstanding expertise in crystal growth [8,9] and post-processing [10–13] of GaN samples has been developed, enabling the production of complex integratable structures.

As integrated photonics emerged as an oncoming new technology to manipulate and process optical signals, GaN's large second-order nonlinear optical coefficients have been exploited to produce second-harmonic-generation devices based on, for example, microdisks [14] and slab waveguides [15–17]. As expected, the design of such devices were supported by several studies on nonlinear optical characterization of GaN's second-order susceptibility [18–21]. Furthermore, GaN-based devices using high-quality resonators [22] and ridge-waveguides [23] were recently demonstrated to exhibit third-order optical nonlinearities, manifested as four-wave mixing. However, the third-order susceptibility of GaN has not been thoroughly characterized yet, especially in the telecommunication spectral range and when excited with femtosecond pulses.

Therefore, we report here a study on both the real and imaginary parts of the third-order nonlinear optical properties of GaN over a broad spectral range, from the visible to the infrared (0.80–2.25 eV; 1550–550 nm), using the femtosecond-laser Z-scan technique. The measured two-photon absorption coefficients and nonlinear refractive indices were compared to values previously reported in the literature aiming to narrow down the wide range of values encountered for these nonlinear optical parameters. In addition, our results were compared with theoretical predictions for direct-gap semiconductors, particularly with models based on the second-order perturbation theory and the Kramers-Kronig relation. The data reported in this work, covering a broad spectral range, is a primary requisite for the proper design and fabrication of nonlinear optical GaN-based devices that rely on its third-order nonlinear optical properties.

## 2. Materials and Methods

The GaN sample used in this study was grown epitaxially by MOVPE on a ~400  $\mu\text{m}$ , double-side-polished 4 inch sapphire substrate. The ~10  $\mu\text{m}$  thick GaN layer was unintentionally n-doped with impurity concentrations  $< 10^{17} \text{ cm}^{-3}$  (details have been described elsewhere [24]). The band gap energy of the MOVPE GaN sample was obtained from its absorption spectrum, which showed a room-temperature band gap of 3.39 eV (365 nm), which is in agreement with other values reported in the literature. In addition, the results demonstrate that the sample does not show any detectable linear absorption at the near infrared excitation wavelengths of the ultrashort pulses used to conduct the experiments.

The spectra of the nonlinear absorption coefficient and the nonlinear refractive index of the GaN sample from the visible to the near-infrared were investigated via open- and closed-aperture Z-scan measurements [25,26], respectively. Both Z-scan techniques were carried out simultaneously by extracting a fraction of the beam from the closed-aperture Z-scan line with a beam splitter to create an open-aperture Z-scan line. Due to this dual-arm configuration, it was possible to remove the nonlinear absorption contribution in the nonlinear refraction measurements and retrieve the pure refractive (closed-aperture) Z-scan signature. As an excitation source, a regenerative chirped pulse amplified Ti:Sapphire laser system (Clark: MXR<sup>®</sup>) was used to pump an Optical Parametric Amplifier (OPA) (TOPAS<sup>®</sup>: Light Conversion) that delivered tunable 120 fs pulses from 0.62 up to 2.7 eV (2000–460 nm). A Gaussian spatial intensity profile was assumed for the laser beam after spatial filtering. Experiments covering a broad spectral range were performed with pulses centered at photon energies in the range of 0.80 to 2.25 eV (1550–550 nm) and pulse energies from 30 to 360 nJ. While the sample was translated along the propagation direction of the laser pulses, its transmission signal was measured using germanium and silicon photodetectors, according to the wavelength range.

Since the Rayleigh range of the beam ( $z_0$ ) of approximately 1 mm is greater than the sample's total length of 430  $\mu\text{m}$ , Z-scan measurements were carried out in the thin sample regime and, therefore, the contribution from the sapphire substrate to the observed nonlinear optical effect had to be removed from the raw data. In order to do that, the nonlinear optical properties of a sapphire substrate that was 600  $\mu\text{m}$  thick were measured for each excitation wavelength prior to measuring the sample with the GaN film. Within the studied energy range from 0.80 to 2.25 eV (1550–550 nm), the sapphire only presented refractive third-order nonlinearities—that is, no nonlinear two-photon absorption was observed [27]. It is also worth mentioning that since optical nonlinearities of fused silica have been extensively characterized [28], the refractive index of fused silica was measured throughout our experiments and compared to reported values to verify its accuracy.

## 3. Results and Discussion

Absorptive and refractive nonlinear optical properties of GaN were measured via the Z-scan technique within the interval of 0.80 to 2.25 eV (1550–550 nm). Representative transmittance curves of open- (left column) and closed-aperture (right column) Z-scan are displayed in Figure 1, specifically for the cases of an excitation energy of 1.77 eV (700 nm) (top row) and 0.88 eV (1400 nm) (bottom

row). Since Z-scan measurements were performed using non-resonant excitation energies in the femtosecond regime, we attributed changes in the transmittance to the manifestation of instantaneous nonlinear absorptive or refractive phenomena. In Figure 1a, the decrease in the measured normalized transmittance (solid circles) of the GaN sample implies the presence of two-photon absorption (2PA). By applying the model proposed by Sheik-Bahae et al. [25] to our experimental data and obtaining the best-fitting curve (solid line), it is possible to determine the material's two-photon absorption coefficient ( $\beta$ ). In our measurements, two-photon absorption was only observed for excitation energies  $\geq 1.77$  eV ( $\lambda \leq 700$  nm). For cases in which the photon energy used was such that 2PA was appreciable, nonlinear refractive measurements (closed-aperture) revealed an asymmetric Z-scan signature with a larger valley amplitude compared to its peak. However, this asymmetry can be removed by calculating the ratio between the raw data from the closed- and open-aperture Z-scan arms, resulting in a symmetrical refractive Z-scan curve, as shown in Figure 1b. For excitation energies lower than 1.77 eV ( $\lambda > 700$  nm), no nonlinear absorption was detected and symmetrical refractive Z-scan curves were obtained, as illustrated in Figure 1c,d for the excitation at 0.88 eV (1400 nm). Analogously to the absorptive case, the nonlinear refractive index of the sample was obtained by finding the best-fitting curve (solid line) also according to the model from the References [25,26].

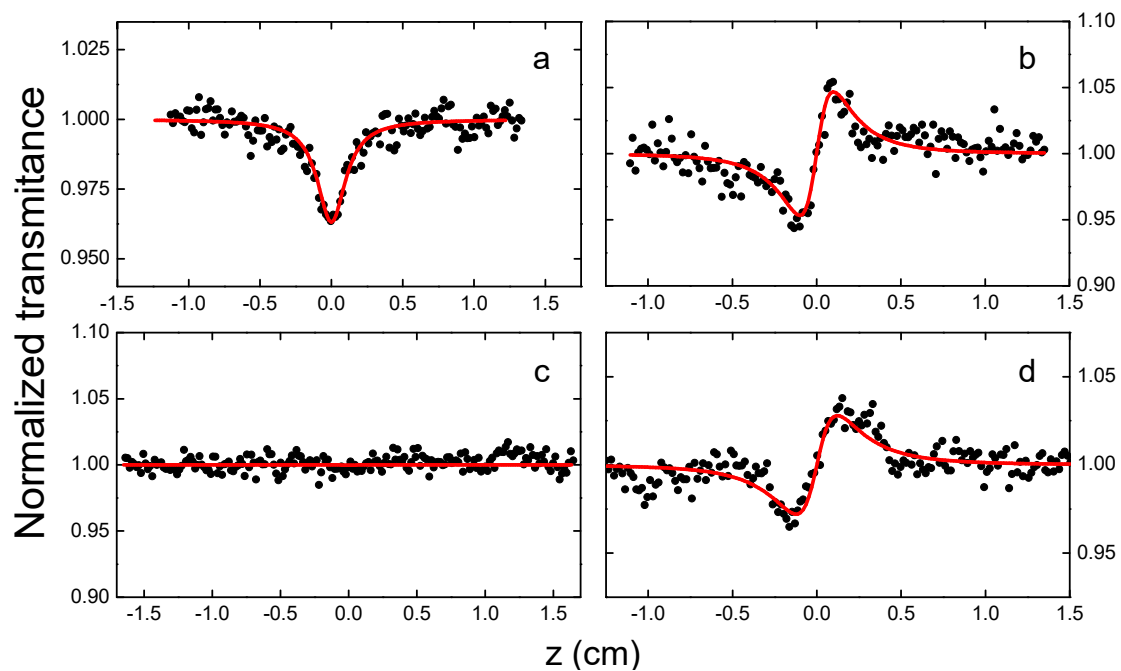


**Figure 1.** Open- and closed-aperture Z-scan signatures and their corresponding fitting curves at 1.77 eV (700 nm) (a,b, respectively) and at 0.88 eV (1400 nm) (c,d, respectively).

The dispersion of the nonlinear coefficients— $\beta$  and  $n_2$ —of GaN over a broad spectral range were obtained by scanning the excitation energies in Z-scan measurements. Throughout our experiments, 2PA was only observed when using photon energies ( $\hbar\omega$ ) from 1.77 to 2.25 eV (700–550 nm), which satisfies the condition  $E_g > \hbar\omega > E_g/2$  (with the experimentally determined band-gap energy  $E_g = 3.39$  eV). Figure 2 reveals an increase of the measured values for  $\beta$  from  $(1.0 \pm 0.2)$  up to  $(2.9 \pm 0.6) \times 10^{-11}$  m/W as the excitation photon energy approaches the linear absorption edge.

A theoretical model for two-photon absorption in the second-order perturbation approach, developed by Sheik-Bahae et al. [29,30], was successfully applied to model the dispersion of optical nonlinearities in wide-gap dielectrics and direct-gap semiconductors. This theory predicts that the value of  $\beta$  as a function of the excitation energy  $E = \hbar\omega$  is given by

$$\beta(\omega) = K \frac{\sqrt{E_p}}{n_0^2 E_g^3} F_2\left(\frac{\hbar\omega}{E_g}\right), \tag{1}$$

where  $F_2(x) = (2x - 1)^{3/2} / (2x)^5$ ,  $n_0$  is the linear refractive index [31], and  $E_p$  is the nearly material independent which has a value of approximately 21 eV. The material-independent constant  $K$  was theoretically calculated to be  $1940 (\times 10^{-11} \text{ m/W})(\text{eV}^{5/2})$  in units where  $E_p$  and  $E_g$  were in electronvolts and  $2 \times 10^{-55}$  in mks units. For materials reported so far, however, the best-fitting of the experimental data was obtained using  $K$  around  $3100 (\times 10^{-11} \text{ m/W})(\text{eV}^{5/2})$  or, as an alternative,  $3.2 \times 10^{-55}$  in mks units [29,30,32–36]. The solid line in Figure 2 represents the best fit of this model that was applied to our experimental data, from which we obtained  $K = (3.0 \pm 0.2) \times 10^3 (\times 10^{-11} \text{ m/W})(\text{eV}^{5/2})$  or  $(3.2 \pm 0.1) \times 10^{-55}$  mks. The good agreement between measurements and theoretical prediction suggests that two-photon absorption is the most dominant effect for nonlinear absorption.

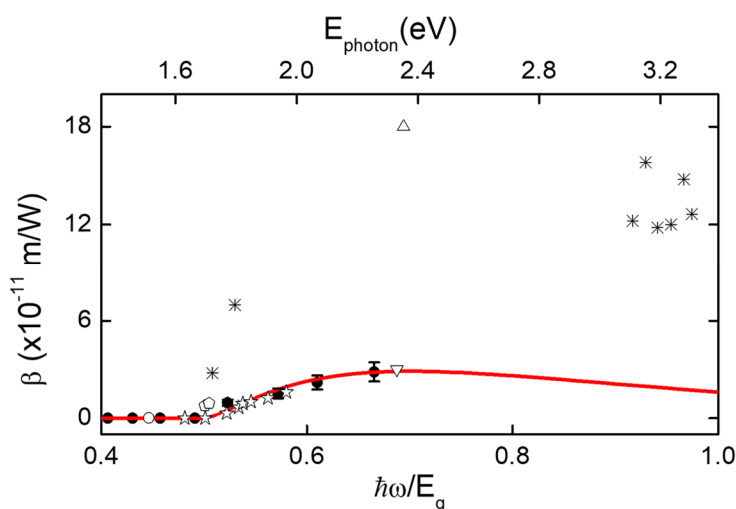


**Figure 2.** Experimental (solid circles) and theoretical (line) dispersion of the two-photon absorption coefficient ( $\beta$ ) of GaN with respect to its band gap energy of 3.39 eV. Literature data are plotted as a hollow circle [37], star [38], pentagons [39], asterisks [40], up-triangle [41], and down-triangle [42].

Previous measurements of GaN’s 2PA coefficient carried out by different methods reported in the literature, at sparse excitation energies or over a shorter spectral range than the one presented here, were incorporated in Figure 2. The values of  $\beta$  are represented as hollow symbols and crosses for better contrast with our experimental data (solid circles). As can be seen in Figure 2, data from Refs. 37 (hollow circle), 38 (star), 39 (pentagons), and 42 (down triangle) agree with our results, as well as with the theoretical prediction. However, values for  $\beta$  reported in Ref. 40 (asterisks) and 41 (up-triangle) differ from the values obtained here. For both cases, the material-independent constant  $K$  is about  $23 \times 10^3 (\times 10^{-11} \text{ m/W})(\text{eV}^{5/2})$  or  $(2.4) \times 10^{-53}$  mks, which is approximately seven times higher than the value observed for GaN and other direct-gap semiconductors. Such higher  $K$  values, for measurements carried out near the one-photon absorption edge ( $\hbar\omega/E_g \sim 1$ ), can be related to excited-state effects that also contribute to nonlinear absorption processes which are different to 2PA.

The nonlinear refractive index dispersion for GaN is displayed in Figure 3 (solid circles). The obtained values for  $n_2$  measured with closed-aperture Z-scan experiments varied from  $(60 \pm 16) \times 10^{-20}$  up to  $(280 \pm 70) \times 10^{-20} \text{ m}^2/\text{W}$ , within the energy range of 0.80 and 2.25 eV ( $\lambda$ : 1550–550 nm;  $\hbar\omega/E_g$ : 0.24–0.66). Additionally, Figure 3 shows results previously reported on the nonlinear refractive index of GaN measured by picosecond and femtosecond Z-scan techniques, represented as hollow symbols, which are in good agreement with the ones measured in this work. Similarly to the two-photon absorption case, there is a theoretical model developed by Sheik-Bahae et al. [29,30] that predicts the dispersion of the real part of the third-order susceptibility

( $\chi^{(3)}$ ) for semiconductors. This model, represented by the solid line in Figure 3, is based on the Kramers-Kronig relation,

$$n_2(\omega) = \frac{c}{\pi} \int_0^\infty \frac{\beta(\omega, \omega')}{\omega'^2 - \omega^2} d\omega'. \tag{2}$$

Considering the dispersion function of the contribution of two-photon absorption ( $G_{2PA}$ ), Raman ( $G_{RAM}$ ) and quadratic Stark effects ( $G_{QSE}$ ), which are explicitly presented in Table 1 for the nondegenerated case [29,30] in Equation (2), and applying the degenerated condition, the final expression for the nonlinear index of refraction in the degenerated case used to model the experimental data is given by

$$n_2(\omega) = K' \frac{\sqrt{E_p}}{n_0^2 E_g^4} G_2 \left( \frac{\hbar\omega}{E_g} \right), \tag{3}$$

in which  $K'$  is a material-independent constant and  $G_2$  is the sum of  $G_{2PA}$ ,  $G_{RAM}$ , and  $G_{QSE}$ .

**Table 1.** Contribution from different effects to the nondegenerate dispersion function  $G_2(x_1, x_2)$  of the nonlinear refractive index [29,30].

Contribution	$G_{(effect)}(x_1, x_2)$
Two-photon absorption (2PA) Raman (RAM)	$H(x_1, x_2) + H(-x_1, x_2)$ $H(x_1, -x_2) + H(-x_1, -x_2)$ where $H(x_1, x_2) = \frac{1}{2^6 x_1^4 x_2^4}$ $\times \left[ \begin{aligned} & \frac{5}{16} x_2^3 x_1^2 + \frac{9}{8} x_2^2 x_1^2 - \frac{9}{4} x_2 x_1^2 - \frac{3}{4} x_2^3 - \frac{1}{32} x_2^3 x_1^2 (1-x_1)^{-3/2} \\ & + \frac{1}{2} (x_2 + x_1)^2 [(1-x_2-x_1)^{3/2} - (1-x_1)^{3/2}] \\ & - \frac{3}{16} x_2^2 x_1^2 [(1-x_1)^{-1/2} + (1-x_2)^{-1/2}] + \frac{3}{2} x_2 x_1^2 (1-x_1)^{1/2} \\ & + \frac{3}{2} x_2^2 x_1 (1-x_1)^{1/2} + \frac{3}{4} x_2 (x_2^2 - x_1^2) (1-x_1)^{1/2} \\ & - \frac{3}{8} x_2^3 x_1 (1-x_1)^{-1/2} + \frac{1}{2} (x_2^2 - x_1^2) [1 - (1-x_2)^{3/2}] \end{aligned} \right]$
Quadratic Stark (QSE)	$\begin{aligned} & \left[ \begin{aligned} & -\frac{1}{2} - \frac{4}{x_1^2} + \frac{4}{x_2^2} - \frac{x_2^2}{x_1} \frac{[(1-x_1)^{-1/2} - (1+x_1)^{-1/2}]}{x_1^2 - x_2^2} \\ & + \frac{2x_1^2(3x_2^2 - x_1^2)}{x_2^2(x_1^2 - x_2^2)^2} [(1-x_2)^{1/2} + (1+x_2)^{1/2}] \\ & - \frac{2x_2^2(3x_1^2 - x_2^2)}{x_1^2(x_1^2 - x_2^2)^2} [(1-x_1)^{1/2} + (1+x_1)^{1/2}] \end{aligned} \right] \\ & \frac{1}{2^9 x_1^4 x_2^4} \left[ \frac{3}{4} \frac{(1-x_1)^{-1/2} - (1+x_1)^{-1/2}}{x_1} - \frac{(1-x_1)^{-3/2} + (1+x_1)^{-3/2}}{8} - \frac{1}{2} \right] \end{aligned}$
$x_1 \neq x_2$	
$x_1 = x_2$	

As one can see in Figure 3,  $n_2$  values from both our experimental data and the literature [39,41,43] are well-fitted by the applied theoretical model, in which the material-independent constant  $K'$  was found to be  $(8.7 \pm 0.5) \times 10^5 (\times 10^{-20} \text{ m/W})(\text{eV}^{7/2})$  in units where  $E_p$  and  $E_g$  are in electronvolts. Alternatively, in mks, such a constant will be given by  $((1.4 \pm 0.1) \times 10^{-79} \text{ mks})$ .

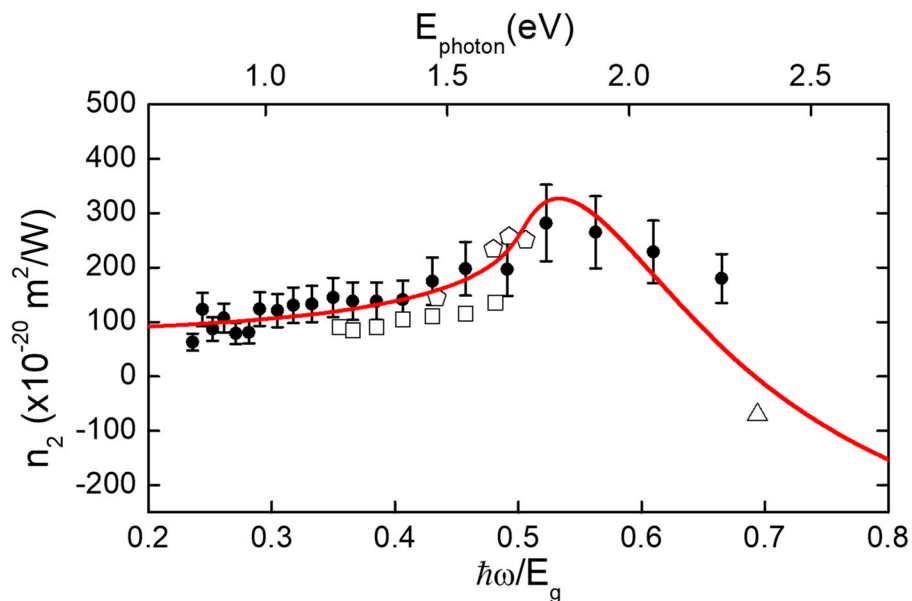


**Figure 3.** Experimental (solid circles) and theoretical (line) dispersion of the nonlinear refractive index ( $n_2$ ) of GaN with respect to its band gap energy of 3.39 eV. Literature data are plotted as pentagons [39], up-triangles [41], and hollow squares [43].

Even though Figure 3 illustrates good agreement between several experimental data sets and the theoretical prediction, a few studies have reported  $n_2$  for GaN orders of magnitude higher than the ones presented here (not shown in Figure 3), for both positive and negative values [23,44,45]. For some of them ( $340 \times 10^{-20} \text{ m}^2/\text{W}$  at 0.80 eV [23] and  $\sim 1 \times 10^{-16} \text{ m}^2/\text{W}$  at 2.33 eV [44]), the difference may be related to the highly indirect experimental method that was used to measure the nonlinear refractive index, such as four-wave mixing experiments, which are susceptible to larger error. For literature reports that, similar to our work, used the closed-aperture Z-scan technique ( $-2.9 \times 10^{-16} \text{ m}^2/\text{W}$  at 3.37 eV [45]), significant discrepancies may arise from the fact that pulses with a high repetition rate (82 MHz) which were centered at energies too close to the one-photon absorption edge have been used. Extreme caution must be taken when measuring refractive nonlinearities at such experimental conditions, mainly because at these energies, linear absorption could be taking place, leading to thermal lensing due to accumulative effects caused by the high repetition rate.

#### 4. Conclusions

In this work, we studied both the real and imaginary parts of the third-order optical nonlinear properties of GaN by using the Z-scan technique at the femtosecond regime over a broad energy range from 0.80 to 2.25 eV (1550–550 nm). The two-photon absorption coefficient ( $\beta$ ) increased from  $(1.0 \pm 0.2)$  up to  $(2.9 \pm 0.6) \times 10^{-11} \text{ m}/\text{W}$  for increasing photon energies, and good agreement with the theoretical model based on the second-order perturbation theory indicates 2PA as the main contribution of the nonlinear absorption. Regarding the nonlinear refractive index dispersion of GaN, our results extended previous data over to the near infrared region, especially at the telecommunication range, measuring  $(90 \pm 30) \times 10^{-20} \text{ m}^2/\text{W}$  at 0.80 eV (1550 nm). Besides that, we observed the decrease of the  $n_2$  values for energies larger than  $\hbar\omega/E_g \sim 0.55$ , an important feature of  $n_2$  dispersion predicted by theory. Thus, information reported here on the third-order nonlinear spectrum of GaN from the visible to the near infrared is important for the development of integrated optoelectronic devices that take advantages from the high optical nonlinearities of GaN.

**Author Contributions:** Conceptualization, C.R.M.; methodology, G.F.B.A., S.N.C.S and J.P.S.; software, G.F.B.A. and C.R.M.; formal analysis, G.F.B.A., S.N.C.S. and C.R.M.; investigation, G.F.B.A., S.N.C.S, J.P.S. and J.D.; resources, C.R.M. and T.V.; data curation, G.F.B.A., S.N.C.S. and J.D.; writing—original draft preparation, G.F.B.A.

and C.R.M.; writing—review and editing, G.F.B.A., S.N.C.S, J.P.S, J.D., T.V. and C.R.M.; supervision, C.R.M.; funding acquisition, C.R.M.

**Funding:** This research was funded FAPESP (2018/11283-7), CNPq and CAPES (Finance Code 001).

**Acknowledgments:** We thank I. Manglano-Clavero, C. Margenfeld, and A. Waag (Institute of Semiconductor Technology, Technische Universität Braunschweig, Germany) for providing the GaN sample.

**Conflicts of Interest:** The authors declare no conflict of interest.

## References

1. Strite, S.; Morkoc, H. GaN, AlN, and InN—A review. *J. Vacuum Sci. Technol. B* **1992**, *10*, 1237–1266. [[CrossRef](#)]
2. Yoder, M. Wide bandgap semiconductor materials and devices. *IEEE Trans. Electron Devices* **1996**, *43*, 1633–1636. [[CrossRef](#)]
3. Monemar, B. Fundamental energy gap of GaN from photoluminescence excitation spectra. *Phys. Rev. B* **1974**, *10*, 676–681. [[CrossRef](#)]
4. Ponce, F.A.; Bour, D.P.; Ponce, F. Nitride-based semiconductors for blue and green light-emitting devices. *Nature* **1997**, *386*, 351–359. [[CrossRef](#)]
5. Huang, Y.; Duan, X.; Cui, Y.; Lieber, C.M. Gallium Nitride Nanowire Nanodevices. *Nano Lett.* **2002**, *2*, 101–104. [[CrossRef](#)]
6. Morkoc, H.; di Carlo, A.; Cingolani, R. GaN-Based Modulation Doped FETs and UN Detectors. *Solid-State Electron.* **2002**, *46*, 157–202. [[CrossRef](#)]
7. Pearton, S.J.; Ren, F. GaN Electronics. *Adv. Mater.* **2000**, *12*, 1571–1580. [[CrossRef](#)]
8. Lei, T.; Ludwig, K.F.; Moustakas, T.D. Heteroepitaxy, polymorphism, and faulting in GaN thin films on silicon and sapphire substrates. *J. Appl. Phys.* **1993**, *74*, 4430–4437. [[CrossRef](#)]
9. Liliental-Weber, Z.; Maltez, R.; Xie, J.; Morkoc, H.; Maltez, R. Propagation of misfit dislocations from AlN/Si interface into Si. *J. Cryst. Growth* **2008**, *310*, 3917–3923. [[CrossRef](#)]
10. Zhou, W.; Min, G.; Song, Z.; Zhang, J.; Liu, Y.; Zhang, J. Enhanced efficiency of light emitting diodes with a nano-patterned gallium nitride surface realized by soft UV nanoimprint lithography. *Nanotechnology* **2010**, *21*, 205304. [[CrossRef](#)]
11. Popa, V.; Tiginyanu, I.; Volciuc, O.; Sarua, A.; Kuball, M.; Heard, P. Fabrication of GaN nanowalls and nanowires using surface charge lithography. *Mater. Lett.* **2008**, *62*, 4576–4578. [[CrossRef](#)]
12. Lee, M.-K.; Kuo, K.-K. Single-step fabrication of Fresnel microlens array on sapphire substrate of flip-chip gallium nitride light emitting diode by focused ion beam. *Appl. Phys. Lett.* **2007**, *91*, 51111. [[CrossRef](#)]
13. Steckl, A.J.; Chyr, I. Focused ion beam micromilling of GaN and related substrate materials (sapphire, SiC, and Si). *J. Vac. Sci. Technol. B Microelectron. Nanometer Struct.* **1999**, *17*, 362. [[CrossRef](#)]
14. Roland, I.; Gromovyi, M.; Zeng, Y.; El Kurdi, M.; Sauvage, S.; Brimont, C.; Guillet, T.; Gayral, B.; Semond, F.; Duboz, J.Y.; et al. Phase-matched second harmonic generation with on-chip GaN-on-Si microdisks. *Sci. Rep.* **2016**, *6*, 34191. [[CrossRef](#)] [[PubMed](#)]
15. Hahn, D.N.; Kiehne, G.T.; Ketterson, J.B.; Wong, G.K.L.; Kung, P.; Saxler, A.; Razeghi, M. Phase-matched optical second-harmonic generation in GaN and AlN slab waveguides. *J. Appl. Phys.* **1999**, *85*, 2497–2501. [[CrossRef](#)]
16. Rigler, M.; Troha, T.; Guo, W.; Kirste, R.; Bryan, I.; Collazo, R.; Sitar, Z.; Zgonik, M. Second-Harmonic Generation of Blue Light in GaN Waveguides. *Appl. Sci.* **2018**, *8*, 1218. [[CrossRef](#)]
17. Xiong, C.; Pernice, W.; Ryu, K.K.; Schuck, C.; Fong, K.Y.; Palacios, T.; Tang, H.X. Integrated GaN photonic circuits on silicon (100) for second harmonic generation. *Opt. Express* **2011**, *19*, 10462–10470. [[CrossRef](#)] [[PubMed](#)]
18. Abe, M.; Sato, H.; Shoji, I.; Suda, J.; Yoshimura, M.; Kitaoka, Y.; Mori, Y.; Kondo, T. Accurate measurement of quadratic nonlinear-optical coefficients of gallium nitride. *J. Opt. Soc. Am. B* **2010**, *27*, 2026–2034. [[CrossRef](#)]
19. Fujita, T.; Hasegawa, T.; Haraguchi, M.; Okamoto, T.; Fukui, M.; Nakamura, S. Determination of Second-Order Nonlinear Optical Susceptibility of GaN Films on Sapphire. *Jpn. J. Appl. Phys.* **2000**, *39*, 2610–2613. [[CrossRef](#)]
20. Sanford, N.A.; Davydov, A.V.; Tsvetkov, D.V.; Dmitriev, A.V.; Keller, S.; Mishra, U.K.; DenBaars, S.P.; Park, S.S.; Han, J.Y.; Molnar, R.J. Measurement of second order susceptibilities of GaN and AlGaIn. *J. Appl. Phys.* **2005**, *97*, 53512. [[CrossRef](#)]

21. Miragliotta, J.; Wickenden, D.K.; Kistenmacher, T.J.; Bryden, W.A. Linear- and nonlinear-optical properties of GaN thin films. *J. Opt. Soc. Am. B* **1993**, *10*, 1447. [[CrossRef](#)]
22. Stassen, E.; Pu, M.; Semenova, E.; Zavarin, E.; Lundin, W.; Yvind, K. High-confinement gallium nitride-on-sapphire waveguides for integrated nonlinear photonics. *Opt. Lett.* **2019**, *44*, 1064–1067. [[CrossRef](#)] [[PubMed](#)]
23. Munk, D.; Katzman, M.; Westreich, O.; Nun, M.B.; Lior, Y.; Siron, N.; Paltiel, Y.; Zadok, A. Four-Wave Mixing and Nonlinear Parameter Measurement in a Gallium-Nitride Ridge Waveguide. *Opt. Mater. Express* **2018**, *8*, 66–72. [[CrossRef](#)]
24. Martins, R.J.; Siqueira, J.P.; Clavero, I.M.; Margenfeld, C.; Fundling, S.; Vogt, A.; Waag, A.; Voss, T.; Mendonca, C.R. Carrier dynamics and optical nonlinearities in a GaN epitaxial thin film under three-photon absorption. *J. Appl. Phys.* **2018**, *123*, 243101. [[CrossRef](#)]
25. Sheik-Bahae, M.; Said, A.; Wei, T.-H.; Hagan, D.; Van Stryland, E.; Hagan, D. Sensitive measurement of optical nonlinearities using a single beam. *IEEE J. Quantum Electron.* **1990**, *26*, 760–769. [[CrossRef](#)]
26. Sheik-Bahae, M.; Said, A.A.; Van Stryland, E.W. High-sensitivity, single-beam  $n_2$  measurements. *Opt. Lett.* **1989**, *14*, 955. [[CrossRef](#)] [[PubMed](#)]
27. Major, A.; Yoshino, F.; Nikolakakos, I.; Smith, P.W.E.; Aitchison, J.S. Dispersion of the nonlinear refractive index in sapphire. *Opt. Lett.* **2004**, *29*, 602. [[CrossRef](#)] [[PubMed](#)]
28. Milam, D. Review and assessment of measured values of the nonlinear refractive-index coefficient of fused silica. *Appl. Opt.* **1998**, *37*, 546–550. [[CrossRef](#)] [[PubMed](#)]
29. Sheik-Bahae, M.; Wang, J.; Van Stryland, E. Nondegenerate optical Kerr effect in semiconductors. *IEEE J. Quantum Electron.* **1994**, *30*, 249–255. [[CrossRef](#)]
30. Sheik-Bahae, M.; Van Stryland, E.W. Optical Nonlinearities in the Transparency Region of Bulk Semiconductors. In *Recent Trends in Thermoelectric Materials Research II*; Elsevier BV: Amsterdam, The Netherlands, 1998; Volume 58, pp. 257–318.
31. Bowman, S.R.; Brown, C.G.; Taczak, B. Optical dispersion and phase matching in gallium nitride and aluminum nitride. *Opt. Mater. Express* **2018**, *8*, 1091–1099. [[CrossRef](#)]
32. Van Stryland, E.W.; Woodall, M.A.; Vanherzeele, H.; Soileau, M.J. Energy band-gap dependence of two-photon absorption. *Opt. Lett.* **1985**, *10*, 490. [[CrossRef](#)] [[PubMed](#)]
33. Vanstryland, E.W.; Vanherzeele, H.; Woodall, M.A.; Soileau, M.J.; Smirl, A.L.; Guha, S.; Boggess, T.F. 2 Photon-Absorption, Nonlinear Refraction, and Optical Limiting in Semiconductors. *Opt. Eng.* **1985**, *24*, 613–623.
34. Sheik-Bahae, M.; Hutchings, D.; Hagan, D.; Van Stryland, E. Dispersion of bound electron nonlinear refraction in solids. *IEEE J. Quantum Electron.* **1991**, *27*, 1296–1309. [[CrossRef](#)]
35. Sheikbahae, M.; Hagan, D.J.; Vanstryland, E.W. Dispersion and Band-Gap Scaling of the Electronic Kerr Effect in Solids Associated with 2-Photon Absorption. *Phys. Rev. Lett.* **1990**, *65*, 96–99. [[CrossRef](#)] [[PubMed](#)]
36. Said, A.; Hagan, D.; Van Stryland, E.; DeSalvo, R.; Sheik-Bahae, M. Infrared to ultraviolet measurements of two-photon absorption and  $n_2$  in wide bandgap solids. *IEEE J. Quantum Electron.* **1996**, *32*, 1324–1333.
37. Streltsov, A.M.; Moll, K.D.; Gaeta, A.L.; Kung, P.; Walker, D.; Razeghi, M. Pulse autocorrelation measurements based on two- and three-photon conductivity in a GaN photodiode. *Appl. Phys. Lett.* **1999**, *75*, 3778–3780. [[CrossRef](#)]
38. Miragliotta, J.; Wickenden, D.K. Transient photocurrent induced in gallium nitride by two-photon absorption. *Appl. Phys. Lett.* **1996**, *69*, 2095–2097. [[CrossRef](#)]
39. Chen, H.; Huang, X.; Fu, H.; Lu, Z.; Zhang, X.; Montes, J.A.; Zhao, Y. Characterizations of nonlinear optical properties on GaN crystals in polar, nonpolar, and semipolar orientations. *Appl. Phys. Lett.* **2017**, *110*, 181110. [[CrossRef](#)]
40. Sun, C.K.; Liang, J.C.; Wang, J.C.; Kao, F.J.; Keller, S.; Mack, M.P.; Mishra, U.; DenBaars, S.P. Two-Photon Absorption Study of GaN. *Appl. Phys. Lett.* **2000**, *76*, 439–441. [[CrossRef](#)]
41. Pacčebutas, V.; Stalnionis, A.; Krotkus, A.; Suski, T.; Perlin, P.; Leszczynski, M. Picosecond Z-scan measurements on bulk GaN crystals. *Appl. Phys. Lett.* **2001**, *78*, 4118–4120. [[CrossRef](#)]
42. Fang, Y.; Zhou, F.; Yang, J.; Wu, X.; Xiao, Z.; Li, Z.; Song, Y. Anisotropy of two-photon absorption and free-carrier effect in nonpolar GaN. *Appl. Phys. Lett.* **2015**, *106*, 131903. [[CrossRef](#)]
43. Fang, Y.; Xiao, Z.; Wu, X.; Zhou, F.; Yang, J.; Yang, Y.; Song, Y. Optical nonlinearities and ultrafast all-optical switching of m-plane GaN in the near-infrared. *Appl. Phys. Lett.* **2015**, *106*, 251903. [[CrossRef](#)]



44. Taheri, B.; Hays, J.; Song, J.J.; Goldenberg, B. Picosecond four-wave-mixing in GaN epilayers at 532 nm. *Appl. Phys. Lett.* **1996**, *68*, 587–589. [[CrossRef](#)]
45. Huang, Y.-L.; Sun, C.-K.; Liang, J.-C.; Keller, S.; Mack, M.P.; Mishra, U.K.; DenBaars, S.P. Femtosecond Z-scan measurement of GaN. *Appl. Phys. Lett.* **1999**, *75*, 3524–3526. [[CrossRef](#)]



© 2019 by the authors. Licensee MDPI, Basel, Switzerland. This article is an open access article distributed under the terms and conditions of the Creative Commons Attribution (CC BY) license (<http://creativecommons.org/licenses/by/4.0/>).